Heliyon 10 (2024) e30658

Contents lists available at ScienceDirect

Heliyon

journal homepage: www.cell.com/heliyon

Research article

Groove design optimization of femoral heads in solid hip implants: Study on stress distribution and total deformation using FEA and full factorial design

Asarudheen Abdudeen, Jaber E. Abu Qudeiri *, Ansar Kareem

Mechanical and Aerospace Engineering Department, College of Engineering, United Arab Emirates University, Al Ain, 15551, United Arab Emirates

ARTICLE INFO

Keywords:
Hip implant
Femoral head
Horizontal grooves
Vertical grooves
Force

ABSTRACT

Hip replacement surgery is a common procedure that relies on the implant's design to withstand daily activities. This study aims to investigate the impact of different surface groove designs on the performance of solid hip implants using finite element analysis (FEA) and optimization techniques. The study evaluates the influence of grooves on the stress distribution and total deformation of the implant, considering three designs: no grooves, horizontal grooves, and vertical grooves on the surface of the femoral head. The simulations were conducted using Ansys Mechanical, and the optimization process was carried out using the general full factorial design method in Minitab software. The results demonstrate that the groove design significantly affects the stress distribution and wear of the implant. The vertical groove design shows better overall results, indicating the best performance. The study also evaluated the influence of force on the performance of the implant, with different load range. The optimization process using the general full factorial design method revealed that the optimal groove design was a vertical model with an optimized groove depth and width. These findings offer valuable insights into the impact of surface groove designs on the performance of solid hip implants, leading to better patient outcomes and longer implant lifespan. Overall, this study provides a comprehensive understanding of the effect of surface groove design on the performance of solid hip implants.

1. Introduction

Total hip replacement surgery is a common orthopaedic procedure that aims to improve the quality of life for individuals who suffer from degenerative hip joint diseases such as osteoarthritis, rheumatoid arthritis, or avascular necrosis [1,2]. One of the key factors that determine the success of the hip replacement surgery is the choice of implant design [3]. The implant should be able to mimic the natural hip joint anatomy and biomechanics, provide adequate support and stability, and minimize wear and tear [4]. Various types of hip implants have been developed over the years, including solid, porous, cemented, and uncemented designs [5].

One of the main challenges in the development of hip implants is to ensure their long-term survival and functionality, particularly in younger and more active patients [6]. One of the factors that can affect the lifespan of hip implants is the wear of the bearing surfaces, which is influenced by the implant design and the patient's activity level [7]. Several studies have investigated the effects of different design parameters on the wear and performance of hip implants, including implant size, material, surface finish, and geometry [8–10].

* Corresponding author.
E-mail address: jqudeiri@uaeu.ac.ae (J.E. Abu Qudeiri).

https://doi.org/10.1016/j.heliyon.2024.e30658
Received 19 September 2023; Received in revised form 20 April 2024; Accepted 1 May 2024
Available online 6 May 2024

One design feature that has received increasing attention in recent years is the use of grooves on the femoral head component of hip implants [1]. Grooves are intended to improve lubrication, reduce contact pressure, and minimize wear between the femoral head and the acetabular cup [11]. However, the optimal groove design parameters, such as depth, width, orientation, and number, are still not fully understood. Previous studies have reported conflicting results regarding the effect of groove design on the performance of hip implants [12–14].

The present study aims to investigate the influence of different groove designs on the performance of a solid hip implant using finite element analysis (FEA) and optimization techniques. In particular, authors focused on the impact of groove depth and width on total deformation, stress distribution, and wear of the implant. Three groove designs were considered, including a femoral head with no grooves, horizontal grooves, and vertical grooves with groove depths of 1 mm and groove widths of 3 mm. Qudeiri et al. [1] have indicated that incorporating grooves on the femoral head's surface, aligned with the dimensions specified, can effectively mitigate friction and wear in hip implants. Fig. 1 shows the three designs of solid femoral head. Fig. 1 (a) Femoral head with vertical grooves, Fig. 1 (b) Femoral head with horizontal grooves Fig. 1 (c) Femoral head with no grooves. Forces of 500 N, 900 N, 1300 N, 1700 N, 2100 N, and 2500 N were applied to all three groove designs of femoral head in the hip implant to find the best design among them. The multistep load from 500 to 2500 N is directly loaded on the top of femoral head. The general full factorial design optimization technique of minitab software was utilized to conduct the optimization process. The results of this study will provide valuable insights into the impact of groove designs on the performance of solid hip implants and can be used to improve the design of hip implants, leading to better patient outcomes and longer implant lifespan.

Study by Qudeiri et al. [15] addressed concerns regarding the design and functionality of grooves featured on the femoral head region, as illustrated in Fig. 1 (b). It is pertinent to clarify that these grooves are not directly exposed to the acetabular cup; rather, a UHMWPE polymer liner serves as a protective intermediary, mitigating the risk of direct metal-to-metal contact and minimizing friction. This design consideration not only ensures the longevity of the implant but also addresses biocompatibility concerns, given the material's compatibility with human tissue. Furthermore, the grooves' configuration facilitates the entrapment of wear particles, thereby enhancing the implant's durability and performance. The numerical model of the femoral head region consists of femoral head of diameter 32 mm made with Ti6Al4V, UHMWPE liner of 7 mm thick and an outer acetabular cup made with same titanium alloy as shown in Fig. 2 (a) and Fig. 2 (b). The model is considered without having any clearance between femoral head and liner. This model is finally simulated using Ansys workbench after applying all the boundary conditions.

Total hip arthroplasty (THA) is a commonly performed surgical procedure for the treatment of hip joint diseases such as osteoarthritis, avascular necrosis, and rheumatoid arthritis [16]. The long-term success of THA depends on various factors such as implant material, implant design, patient activity level, and surgical technique. One of the critical factors that affect the performance of hip implants is the design of the femoral head. The femoral head is the ball-shaped component of the hip implant that articulates with the acetabulum, a concave socket-shaped structure in the pelvis. The design of the femoral head, particularly the presence of grooves, can significantly affect the load distribution, wear, and total deformation of the implant [17,18].

Numerous studies have investigated the effect of groove design on the performance of hip implants. Some studies have shown that grooves can reduce the risk of dislocation by increasing the range of motion [19,20], while others have demonstrated that grooves can increase the contact stress and wear of the implant [21,22]. Grooves are commonly added to the femoral head to enhance the stability of the implant by increasing the contact area and promoting bone ingrowth [23]. Moreover, recent research by Gandhi et al. [24] highlighted the significance of groove geometry in mitigating implant-related complications. They found that a specific combination of groove depth and width substantially improved implant stability and reduced the likelihood of post-operative complications. Similarly, a study by Zhou M et al. [25] underscored the importance of groove parameters in optimizing implant performance, emphasizing the role of groove shape in reducing wear and friction. Additionally, Moghadasi K et al. [26] conducted a comparative analysis of various groove designs, emphasizing the need for further exploration of groove dimensions to minimize implant wear and maximize long-term performance. These findings collectively emphasize the ongoing controversy surrounding optimal groove design and underscore the necessity of investigating groove parameters, such as depth and width, to elucidate their impact on the performance of hip

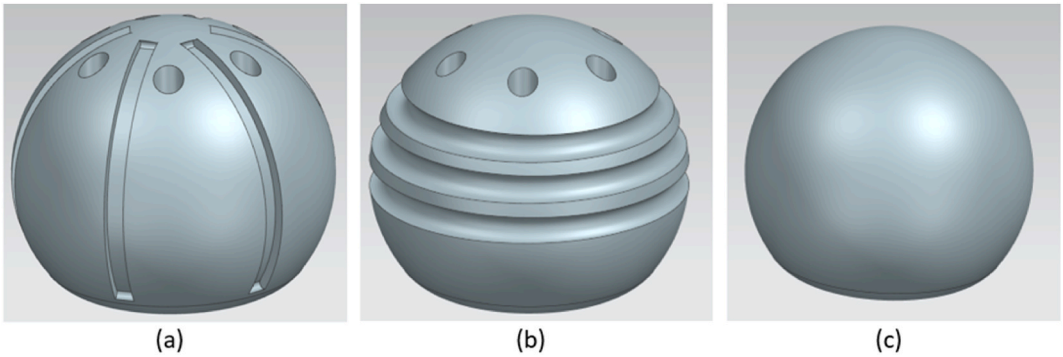

Fig. 1. (a–c): Designs of solid femoral head (a) Femoral head with vertical grooves (b) Femoral head with horizontal grooves (c) Femoral head with no grooves.

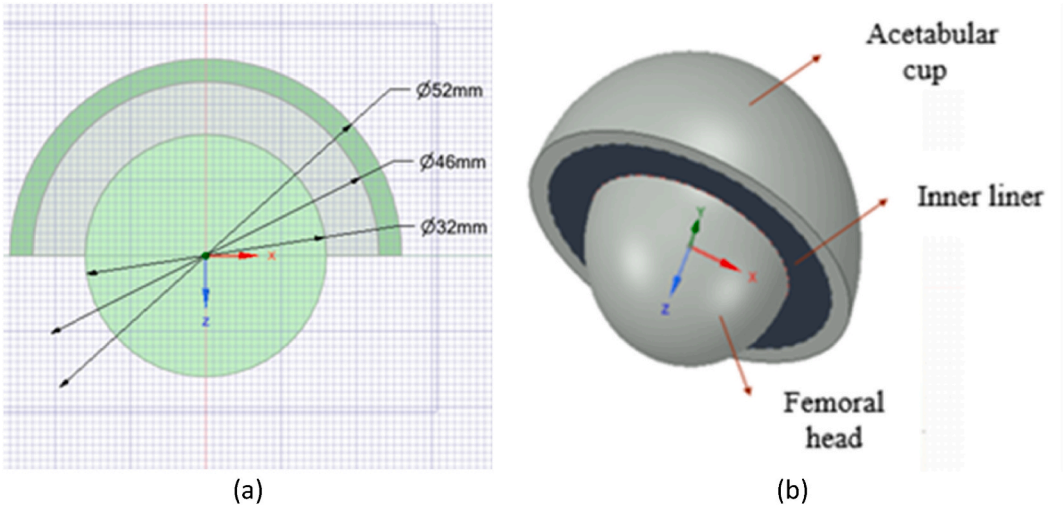

Fig. 2. a) cross sectional view of femoral head, liner and acetabular cup and b) 3D model of femoral head region [15].

implants. Therefore, the optimal groove design remains controversial, and it is essential to investigate the impact of groove parameters such as depth and width on the performance of hip implants.

Finite element analysis (FEA) is a powerful tool for investigating the mechanical behaviour of hip implants. FEA can simulate the contact between the femoral head and the acetabulum and provide valuable insights into the stress distribution, wear, and deformation of the implant [2,27]. Various studies have used FEA simulations to investigate the effect of groove designs on the femoral head of hip implants. For example, Muratoglu et al. [28] compared the wear and deformation of hip implants with different surface finishes in a dynamic hip simulator. They found that rougher surfaces had higher wear rates and more significant deformation than smoother surfaces. Hussain et al. [29] used the Taguchi method to design a novel lubricating groove in hip implants. They found that the optimized groove design reduced the contact pressure and wear of the implant. Optimization techniques such as the full factorial design method can also be used to identify the optimal groove design that maximizes the performance of hip implants [30,31]. The general full factorial design is a statistical method used to evaluate the effect of multiple factors on the outcome of the design. Previous studies have used the general full factorial design to optimize the design of hip implants. For example, Goshulak et al. [32] used the general full factorial design to optimize the design of a hip implant with a novel lubricating groove. The study found that the groove design improved the lubrication of the implant, reducing friction and wear.

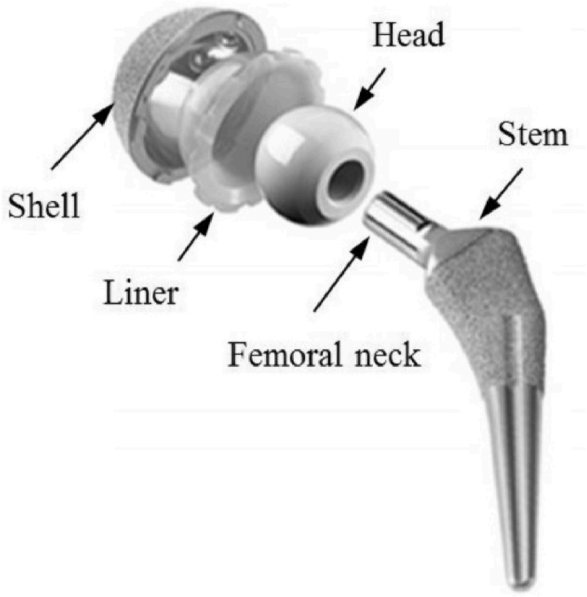

Fig. 3. Components of an artificial hip Joint [37].

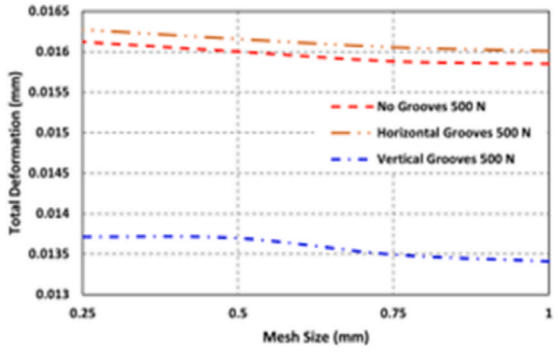

(a)

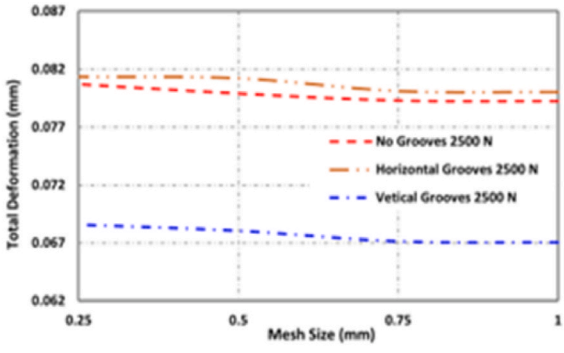

(b)

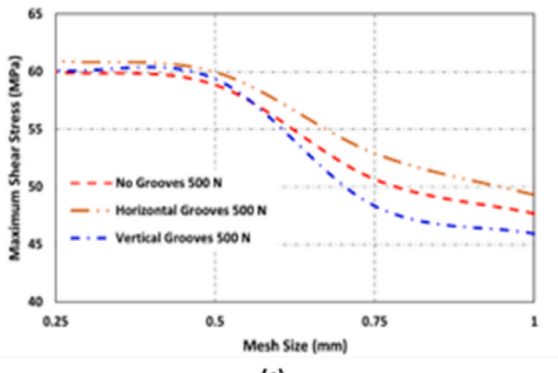

(c)

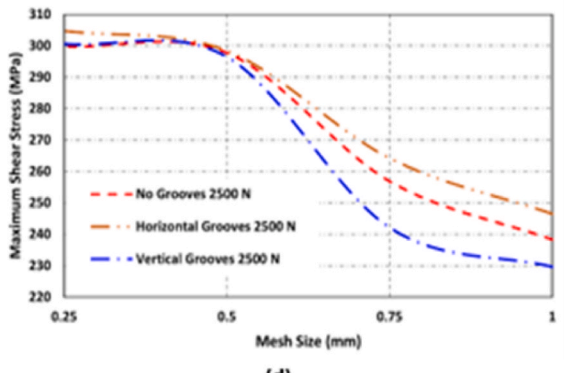

(d)

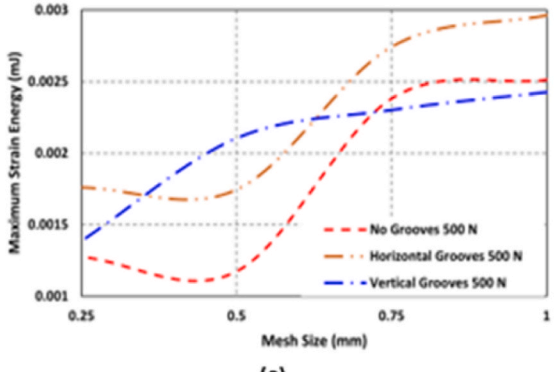

(e)

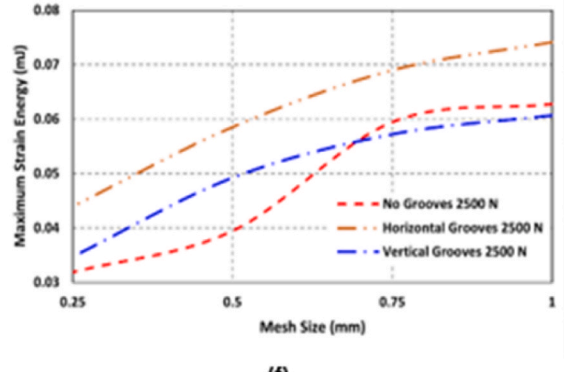

(f)

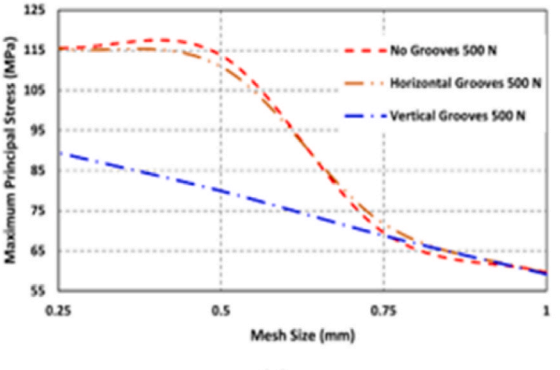

(g)

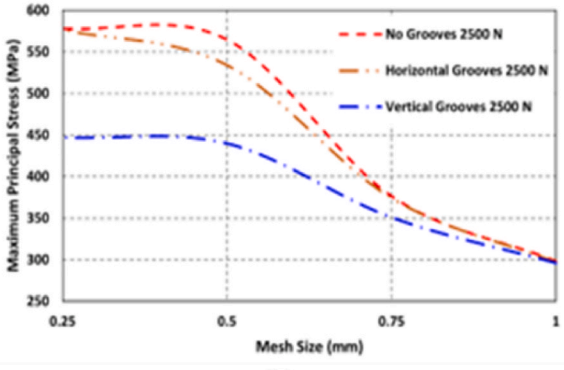

(h)

(caption on next page)

Fig. 4. Convergence Analysis for Loads of 500 N and 2500 N (a) Total Deformation (mm) Vs Mesh Size (mm) for 500 N (b) Total Deformation (mm) Vs Mesh Size (mm) for 2500 N (c) Maximum Shear Stress (MPa) Vs Mesh Size (mm) for 500 N (d) Maximum Shear Stress (MPa) Vs Mesh Size (mm) for 2500 N (e) Maximum Strain Energy (mJ) Vs Mesh Size (mm) for 500 N (f) Maximum Strain Energy (mJ) Vs Mesh Size (mm) for 2500 N (g) Maximum Principal stress (MPa) Vs Mesh Size (mm) for 500 N (h) Maximum Principal stress (MPa) Vs Mesh Size (mm) for 2500 N.

Several recent studies have investigated the impact of groove design on the performance of hip implants using FEA and optimization techniques. For example, Huang et al. [33] investigated the effect of groove width and depth on the contact stress and wear of hip implants using FEA and Taguchi optimization method. They found that the optimal groove design was a 3 mm wide and 1 mm deep groove, which resulted in the lowest wear and contact stress. Similarly, Zhao et al. [34] used FEA and response surface methodology to investigate the effect of groove width and depth on the contact stress and wear of hip implants. They found that a groove width of 2 mm and depth of 1 mm resulted in the lowest contact stress and wear. Lee J et al. [35] studied the effect of groove depth and width on the stress distribution and contact area of a femoral head implant using FEA. They found that increasing the groove depth and width resulted in a significant reduction in stress concentration and an increase in contact area. Regarding the material combination, many authors including Abdudeen et al. [36] has mentioned that Ti–6Al–4V is the best material used for making acetabular cup, femoral head and stem and ultra-high molecular weight polyethylene (UHMWPE) plastic is best for the inner liner. The components of an artificial hip joint are shown in Fig. 3.

Overall, the literature suggests that groove design significantly affects the performance of hip implants, and optimization techniques can be used to identify the optimal groove design that maximizes the performance of the implant. The present study aims to investigate the impact of groove design on the stress distribution and total deformation of solid hip implants using FEA and full factorial design optimization method.

In this section, a concise overview of the paper's organization is provided to guide the reader through the subsequent sections. The paper is structured as follows: Section 2, Materials and Methods, elaborates on the methodology employed in this study, describing the materials used, simulation techniques, and optimization approach in detail. Section 3, Results and Discussion, presents the outcomes of simulations and optimization efforts, analysing and interpreting these results and providing insights into the performance of various groove designs. Within Section 3, subsections titled Simulation and Optimization offer in-depth explanations of the factors contributing to the superior performance of the femoral head with different groove designs. Section 4, Conclusion, summarizes the key findings of the study and discusses their implications for the field of hip implant design, highlighting the study's limitations and suggesting avenues for future research.

2. Materials and methods

To investigate the impact of groove designs on the performance of solid hip implants, a computational simulation approach was employed. The methodology involved four main steps: (1) CAD modelling of the femoral head, acetabular cup, liner and femoral stem (2) finite element analysis (FEA) using Ansys Mechanical software, (3) optimization using general full factorial design in Minitab software, and (4) post-processing of the simulation results.

CAD modelling: The CAD model of the hip implant was created and assembled using Siemens Nx 2021 modelling software. The femoral head was designed as a solid sphere with a diameter of 32 mm, while the acetabular cup was modelled as a hemispherical cup with an inner diameter of 46 mm. Groove design was chosen as vertical, horizontal, no grooves model with a groove depth of 1 mm and a width of 3 mm. The outer diameter of the liner is same as the inner diameter of the cup. The components were assembled in their natural anatomical position, with the centre of the femoral head aligned with the centre of the acetabular cup, the liner in between the acetabular cup and femoral head, and femoral stem attached with the bottom of the femoral head.

FEA simulation: Ansys 2022/R2 Mechanical software was used to perform FEA simulations of the model. The simulation was conducted under six different loading conditions, ranging from 500 N to 2500 N, with increments of 400 N. The femoral head, stem and acetabular cup was assumed to be rigid made of Ti–6Al–4V with 4.5 kg/m^3 density, while the liner was modelled as a linear elastic material named UHMWPE with a Young's modulus of 927.9 MPa and Poisson's ratio of 0.4. The contact between the femoral head and acetabular cup was simulated using a frictionless contact algorithm, and the simulation was run for a total of 10,000 cycles. A total of 18 simulations were run, corresponding to all possible combinations of groove design and applied force.

Sensitivity Analysis: A sensitivity analysis was conducted to investigate the effect of varying the mesh size on the FEA results. The mesh size was varied from 0.25 mm to 1 mm, and the resulting total deformation, maximum shear stress, maximum strain energy, and maximum principal stress values were compared. The ideal mesh size was chosen as 0.25 mm. Convergence history after the meshing sensitivity analysis is shown in Fig. 4(a–h). Fig. 4(a–h) shows the Convergence Analysis for Loads of 500 N and 2500 N (a) Total Deformation (mm) Vs Mesh Size (mm) for 500 N (b) Total Deformation (mm) Vs Mesh Size (mm) for 2500 N (c) Maximum Shear Stress (MPa) Vs Mesh Size (mm) for 500 N (d) Maximum Shear Stress (MPa) Vs Mesh Size (mm) for 2500 N (e) Maximum Strain Energy (mJ) Vs Mesh Size (mm) for 500 N (f) Maximum Strain Energy (mJ) Vs Mesh Size (mm) for 2500 N (g) Maximum Principal stress (MPa) Vs Mesh Size (mm) for 500 N (h) Maximum Principal stress (MPa) Vs Mesh Size (mm) for 2500 N.

This Fig. 4 presents the convergence analysis results for two load conditions: 500 N and 2500 N. Various mesh sizes, ranging from 1 (coarsest) to 0.25 (finest), were employed in the simulation. The graph illustrates the convergence behaviour of critical mechanical parameters, including Total Deformation, Maximum Shear Stress, Maximum Strain Energy, and Maximum Principal Stress, for these load conditions. Notably, mesh sizes 0.25 and 0.5 exhibit close alignment in results, signifying convergence, while mesh sizes 0.75 and

1 demonstrate discernible discrepancies. These findings underscore the significance of selecting an appropriate mesh size to ensure precise and dependable simulation outcomes for varying loads.

Fig. 5 displays the detailed part geometry used in this study, with a mesh size of 0.25 mm. The finer mesh allows for a more accurate representation of the component's intricate features and provides insights into how the meshing captures critical regions. Pay particular attention to areas of interest, such as stress concentration points, contact surfaces, and regions prone to deformation, as these aspects are crucial for understanding the mechanical behaviour of the analysed structure.

Optimization: The optimization process was performed using general full factorial design in Minitab software. The parameters considered were groove design and force, and three designs were evaluated: a femoral head with no grooves, horizontal grooves, and vertical grooves.

Post-processing: The results of the FEA simulations were analysed to evaluate the performance of each groove design in terms of total deformation, stress distribution, and wear. The maximum total deformation, maximum shear stress, maximum strain energy, and maximum principal stress were calculated for each simulation. Further analysis and optimization were carried out using Mini tab general full factorial design technique.

3. Result and discussion

3.1. Simulation

The results of the static structural analysis of the hip implant under different loading conditions are presented in this section. The analysis provided detailed insights into the stress and strain distribution in the different components of the implant, which can inform the design of more effective and safer implants.

In this study, authors conducted a static structural analysis of a hip implant using Ansys Mechanical 2022 R2 software to gain a better understanding of its mechanical behaviour under different loading conditions. The finite element model of the hip implant included four components: an acetabular cup, liner, femoral head, and femoral stem, with a total volume of 49194 mm^3 and a mass of 0.18325 kg. The material properties of the components were chosen based on their commonly used materials in hip implant design: UHMWPE plastic for the liner, and Ti–6Al–4V for the rest of the parts. To determine the ideal mesh size, researchers have conducted a sensitivity analysis and created a model with 2543275 nodes and 1494570 elements using an element size of 0.25 mm with adaptive sizing techniques enabled. Then performed a total of six loading conditions, ranging from 500 N to 2500 N in increments of 400 N, applied in both the horizontal and vertical directions, with the femoral stem having fixed support, and the environmental temperature set to 22 °C throughout. The simulation was conducted for 10,000 steps to capture the behaviour of the hip implant under the loading conditions. The results showed that the hip implant was able to withstand the applied loads without failure, and the stresses in the different components were within acceptable limits. However, authors have observed areas of high stress concentration in the femoral stem and acetabular cup, which may lead to fatigue failure over time.

The results obtained from simulation are indicated below. Fig. 6(a–d) shows the values of (a) maximum total deformation (mm), (b) maximum shear stress (MPa), (c) maximum strain energy (mJ) and (d) maximum principal stress (MPa) for solid hip implant with vertical grooves on femoral head under the force of 500 N. Fig. 7(a–d) shows the values of (a) maximum total deformation (mm), (b) maximum shear stress (MPa), (c) maximum strain energy (mJ) and (d) maximum principal stress (MPa) for solid hip implant with

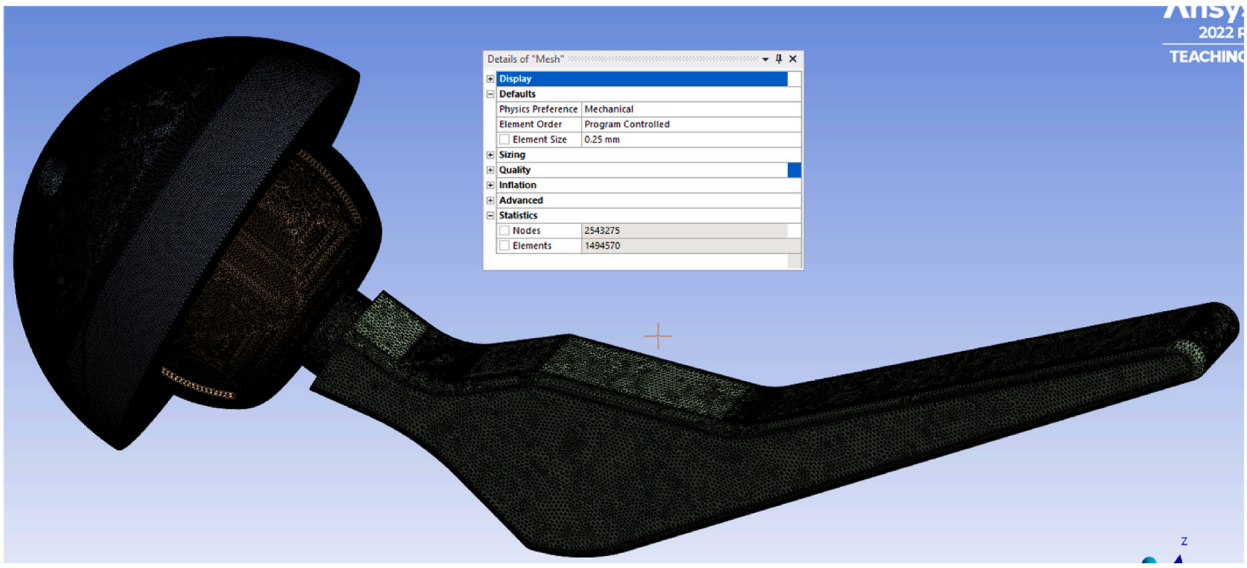

Fig. 5. Part geometry with 0.25 mm mesh size.

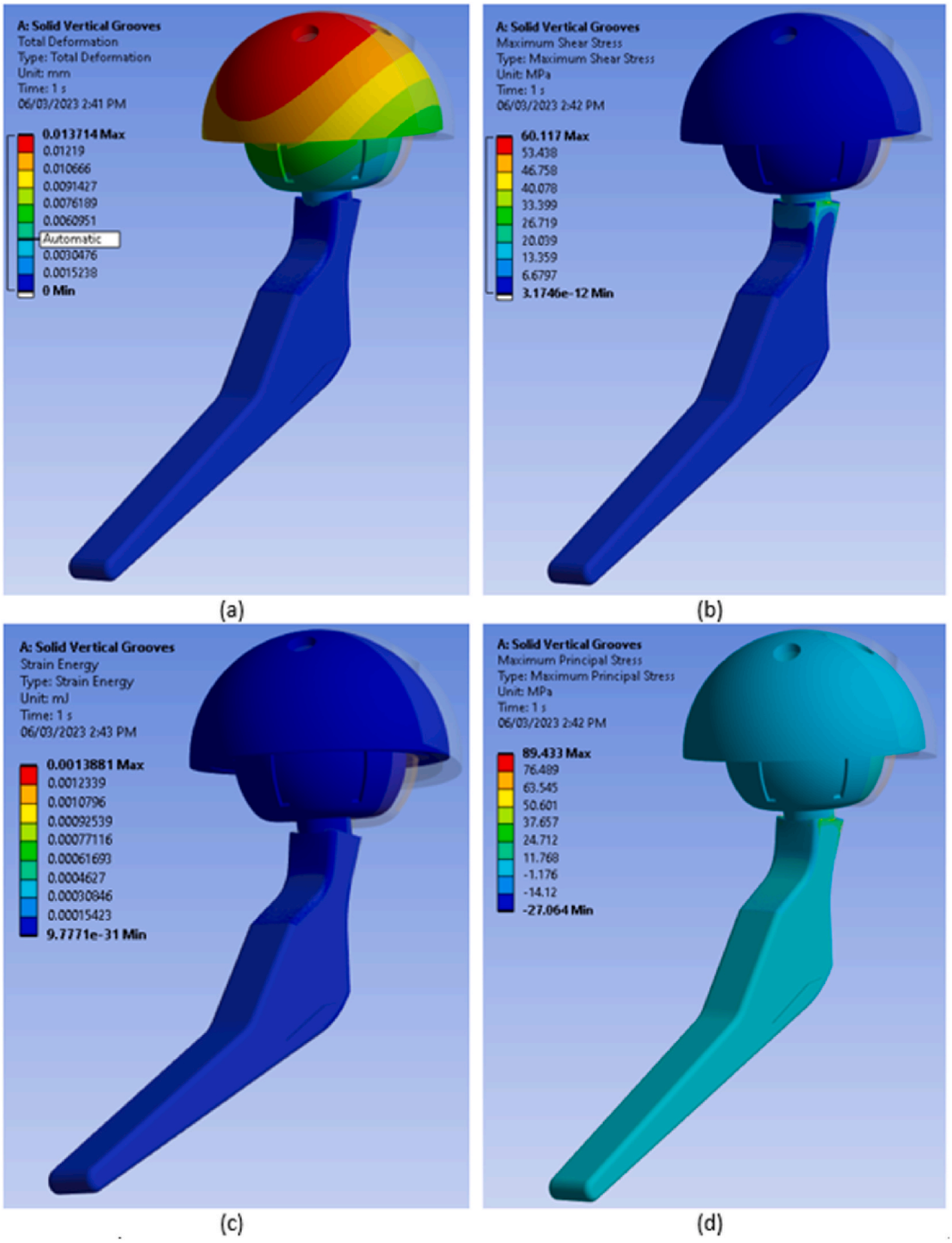

Fig. 6. (a) Total Deformation Maximum (mm) (b) Maximum Shear Stress (MPa) (c) Maximum Strain Energy (mJ) (d) Maximum Principal stress (MPa) for solid hip implant with vertical grooves on femoral head under 500 N.

horizontal grooves on femoral head under the force of 500 N. Fig. 8(a–d) shows the values of (a) maximum total deformation (mm), (b) maximum shear stress (MPa), (c) maximum strain energy (mJ) and (d) maximum principal stress (MPa) for solid hip implant with no grooves on femoral head under the force of 500 N.

Similarly, Fig. 9(a–d) shows the values of (a) maximum total deformation (mm), (b) maximum shear stress (MPa), (c) maximum strain energy (mJ) and (d) maximum principal stress (MPa) for solid hip implant with vertical grooves on femoral head under the force of 2500 N. Fig. 10(a–d) shows the values of (a) maximum total deformation (mm), (b) maximum shear stress (MPa), (c) maximum strain energy (mJ) and (d) maximum principal stress (MPa) for solid hip implant with horizontal grooves on femoral head under the

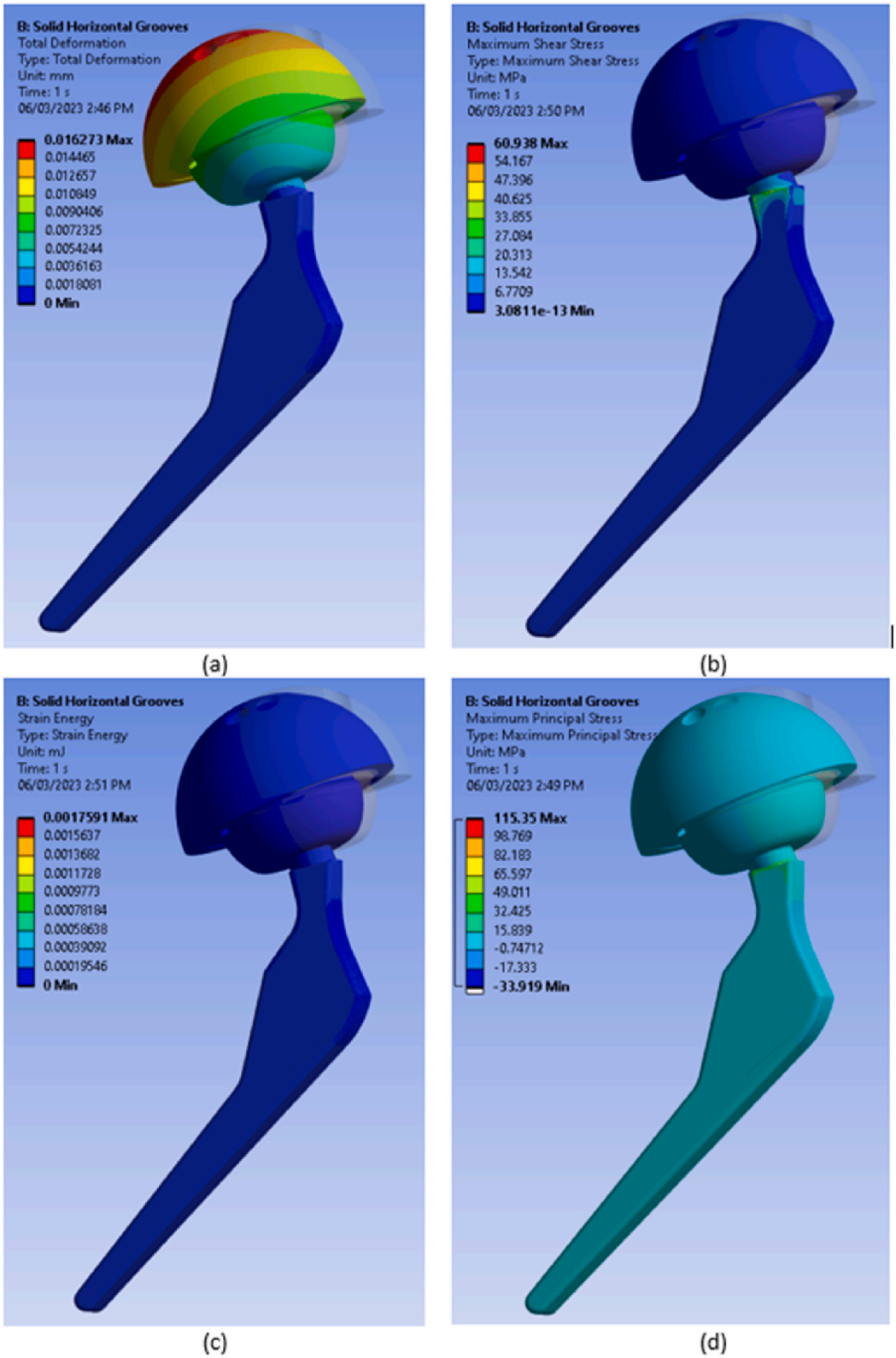

Fig. 7. (a) Total Deformation Maximum (mm) (b) Maximum Shear Stress (MPa) (c) Maximum Strain Energy (mJ) (d) Maximum Principal stress (MPa) for solid hip implant with horizontal grooves on femoral head under 500 N.

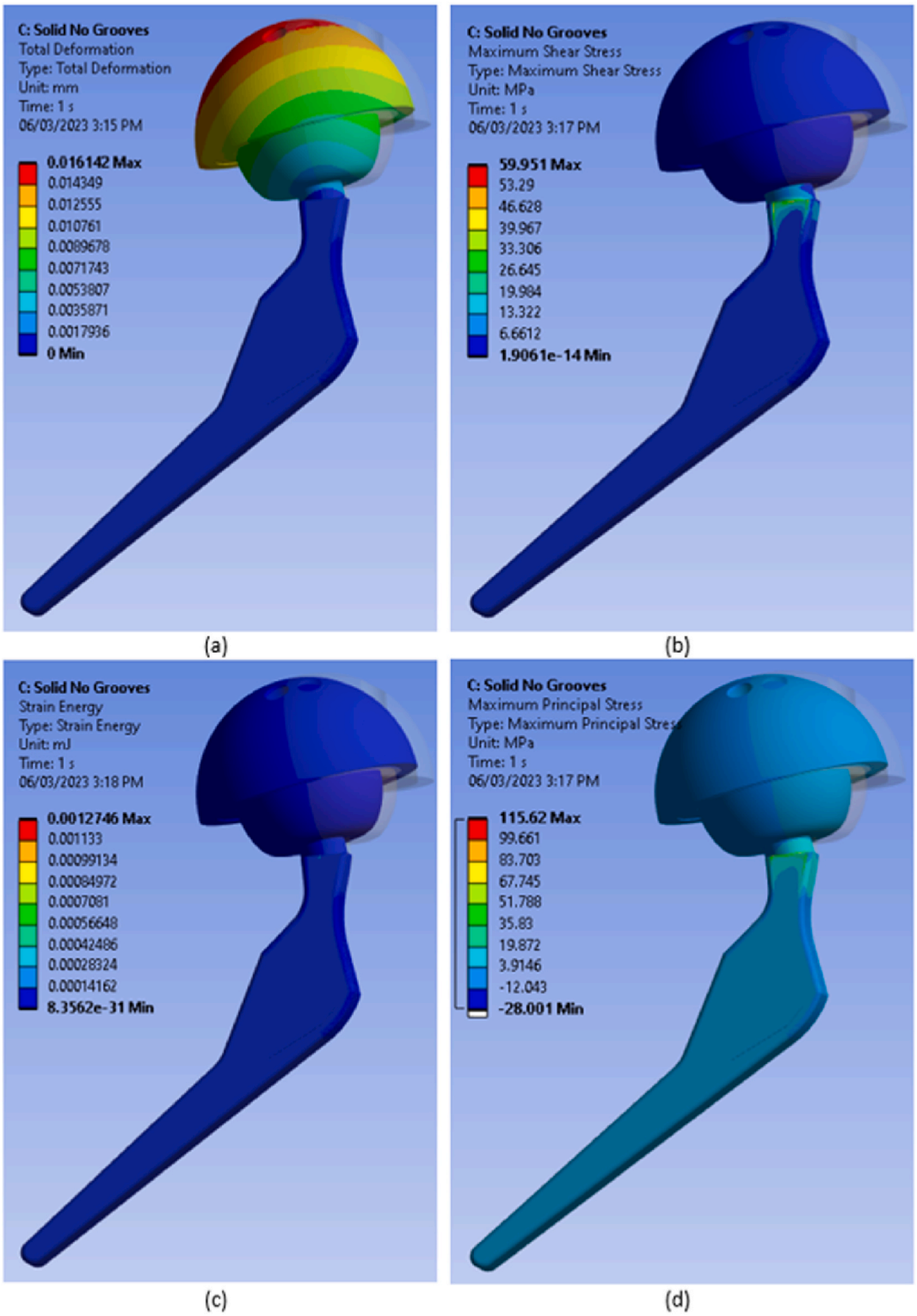

Fig. 8. (a) Total Deformation Maximum (mm) (b) Maximum Shear Stress (MPa) (c) Maximum Strain Energy (mJ) (d) Maximum Principal stress (MPa) for solid hip implant with no grooves on femoral head under 500 N.

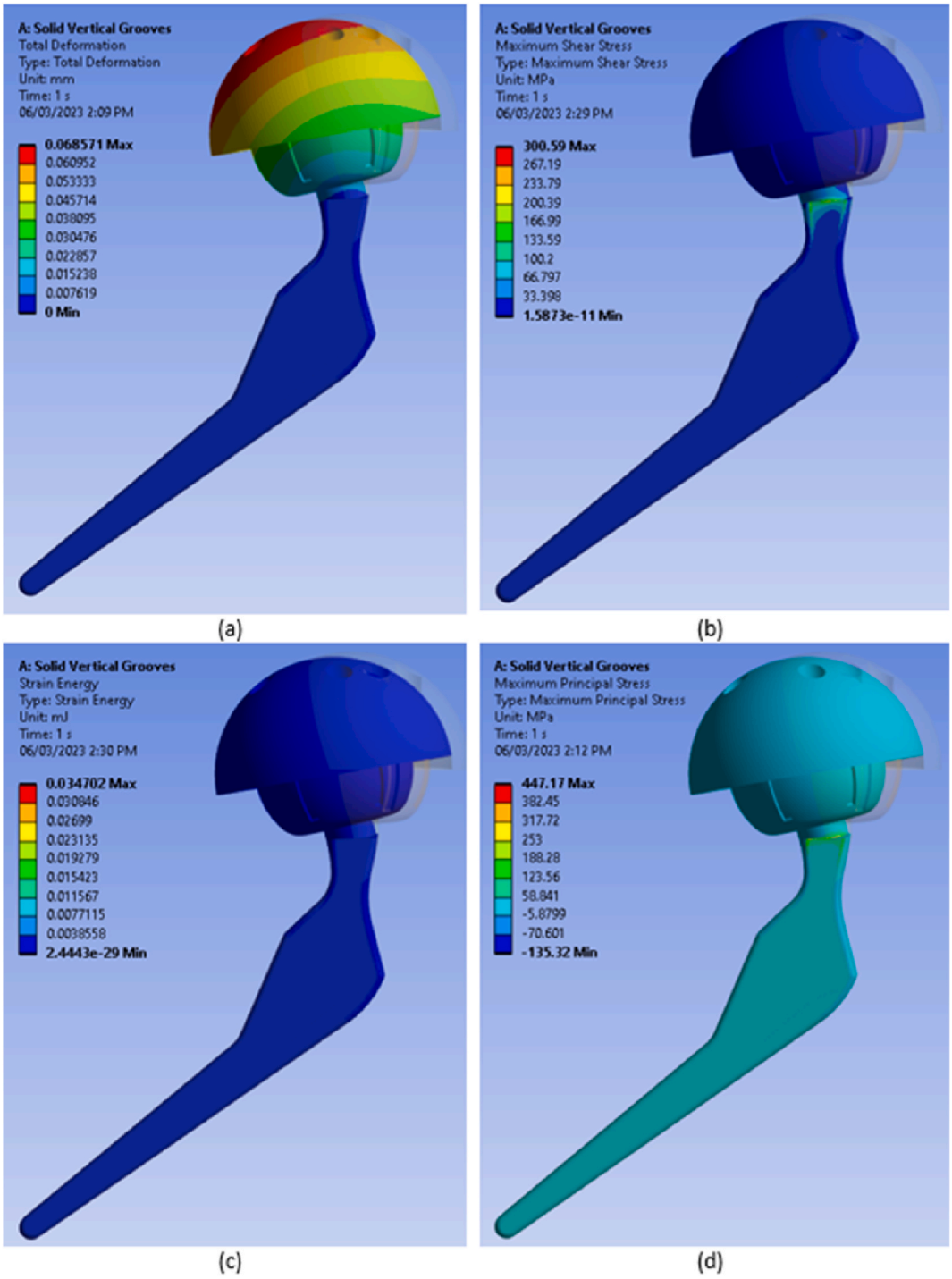

Fig. 9. (a) Total Deformation Maximum (mm) (b) Maximum Shear Stress (MPa) (c) Maximum Strain Energy (mJ) (d) Maximum Principal stress (MPa) for solid hip implant with vertical grooves on femoral head under 2500 N.

force of 2500 N. Fig. 11(a–d) shows the values of (a) maximum total deformation (mm), (b) maximum shear stress (MPa), (c) maximum strain energy (mJ) and (d) maximum principal stress (MPa) for solid hip implant with no grooves on femoral head under the force of 2500 N.

The research study involved 18 simulations to analyse the mechanical behaviour of different hip implant designs. The simulations were conducted with forces ranging from 500 N to 2500 N, in increments of 400 N, for each case of femoral head having vertical

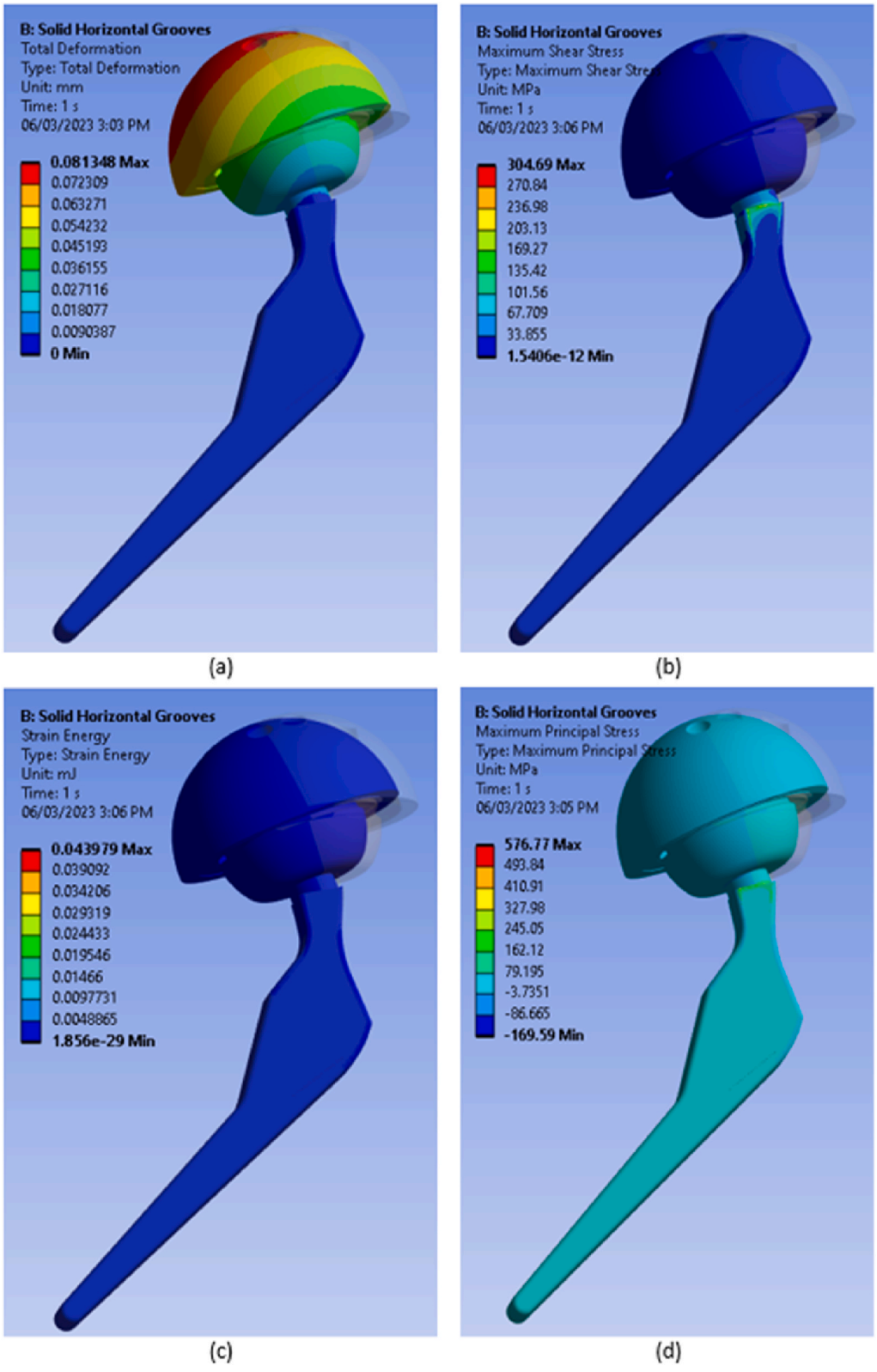

Fig. 10. (a) Total Deformation Maximum (mm) (b) Maximum Shear Stress (MPa) (c) Maximum Strain Energy (mJ) (d) Maximum Principal stress (MPa) for solid hip implant with horizontal grooves on femoral head under 2500 N.

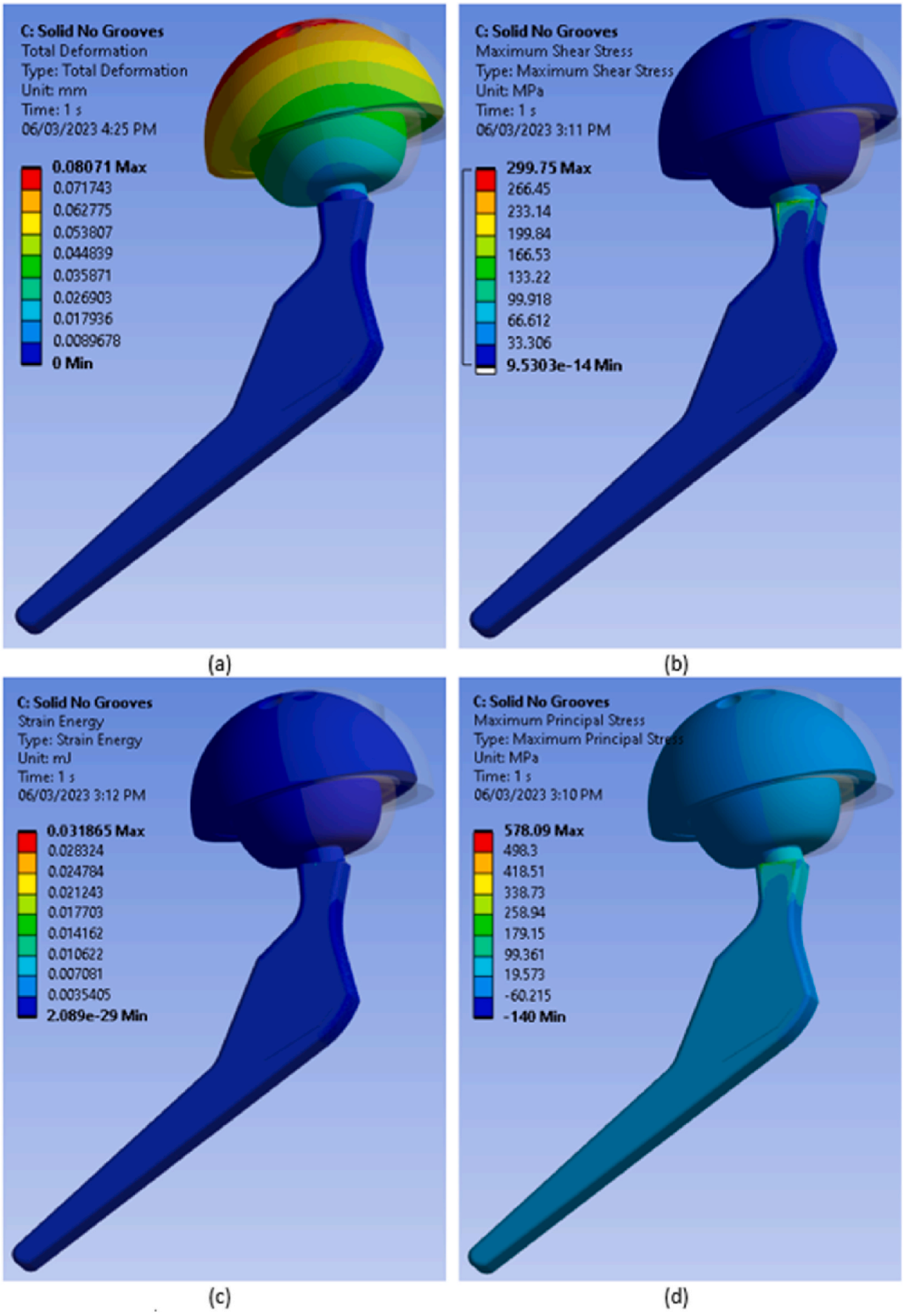

Fig. 11. (a) Total Deformation Maximum (mm) (b) Maximum Shear Stress (MPa) (c) Maximum Strain Energy (mJ) (d) Maximum Principal stress (MPa) for solid hip implant with no grooves on femoral head under 2500 N.

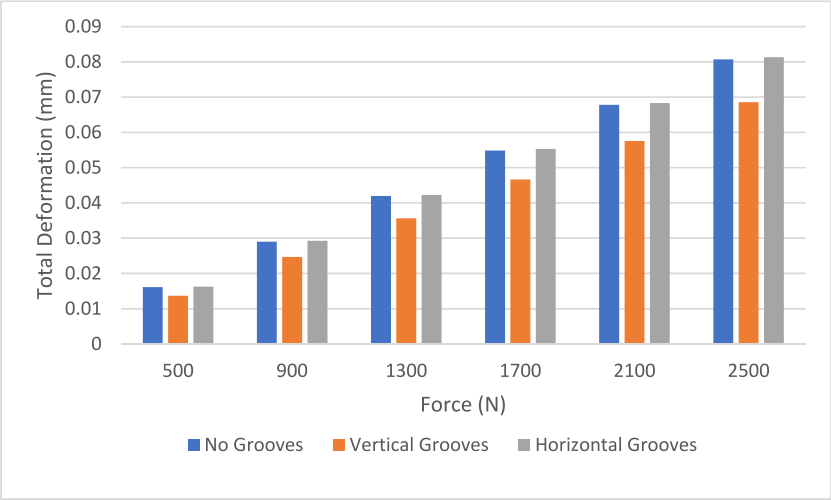

Fig. 12. Total deformation (mm) Vs force (N).

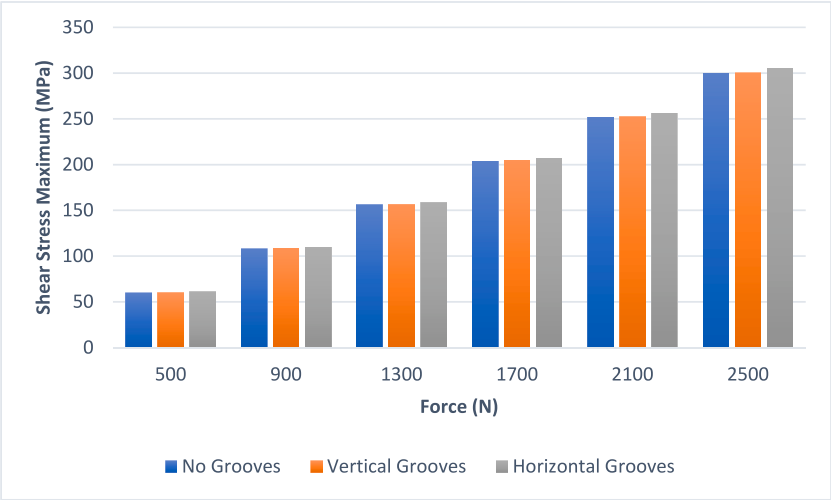

Fig. 13. Shear stress maximum (MPa) Vs force (N).

grooves, horizontal grooves, and no grooves in a completely solid hip implant. The results of the simulations were analysed based on four parameters: maximum total deformation (mm), maximum shear stress (MPa), maximum strain energy (mJ), and maximum principal stress (MPa). The graphs presented in Figs. 12–15 illustrate the values of these parameters for each of the three groove designs under the specified range of forces.

Fig. 12 shows the total deformation (mm) versus force (N) for all three groove designs under the range of forces tested. It can be observed that the maximum total deformation increases linearly with an increase in force for all three designs. However, results shows that the vertical grooves design consistently had lower mean deformation values as compared to the other groove designs. Hence implant with vertical groove design will undergoes less change in shape due to the application of force.

Fig. 13 illustrates the maximum shear stress (MPa) versus force (N) for all three groove designs. The results indicate that the maximum shear stress values for all three designs remain relatively constant with increasing force. There were no significant differences observed in the maximum shear stress values among the three groove designs. P value obtained from the statistical analysis mentioned in Table 3 shows that the differences occurred are not significant and could have occurred due to random reasons.

Fig. 14 presents the maximum strain energy (mJ) versus force (N) for all three groove designs. The horizontal grooves design consistently had the highest mean strain energy values, indicating that this design has the ability to absorb more energy under loading conditions. Interestingly, the vertical grooves design had higher mean strain energy values compared to the solid femoral head having no grooves, indicating that the vertical grooves design may have some potential benefits in terms of energy absorption. The difference in strain energy, particularly the higher values associated with horizontal grooves compared to vertical grooves and no grooves, can be attributed to several design-related factors. Horizontal grooves tend to increase the contact area between the femoral head and the

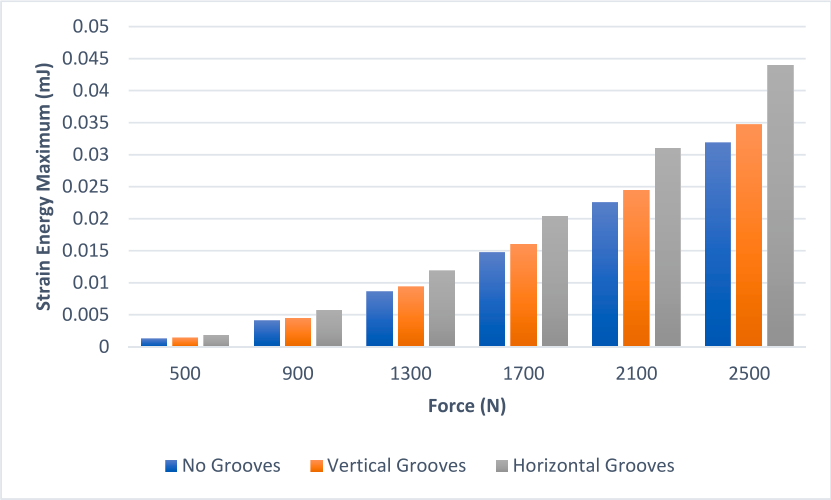

Fig. 14. Strain energy maximum (mJ) Vs force (N).

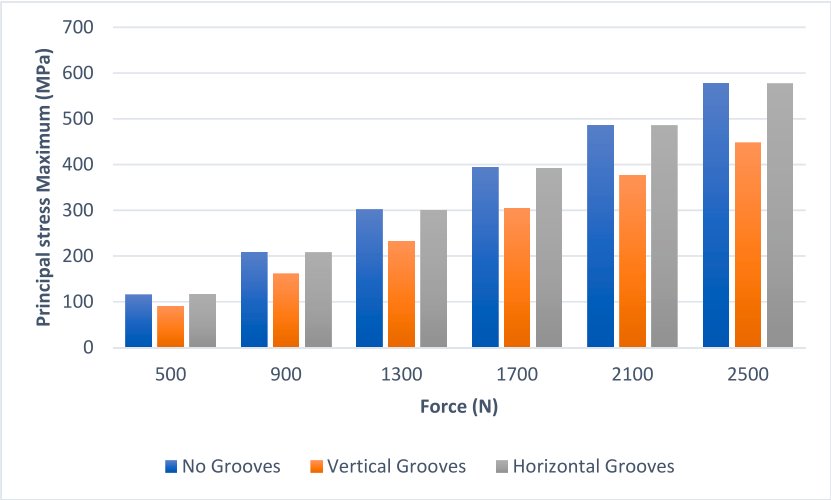

Fig. 15. Principal stress maximum (MPa) Vs force (N).

acetabular cup. This broader contact area distributes the load more evenly, potentially reducing localized stress and strain concentrations. Groove orientation plays a crucial role in how the load is distributed across the implant's surface. Horizontal grooves may offer a more balanced distribution of forces during activities like walking and running. The orientation of grooves can affect lubrication and friction. Horizontal grooves may enhance lubrication and reduce friction, leading to lower frictional forces and, consequently, decreased strain energy. The mechanical properties of the implant material interact with groove design. Horizontal grooves may align more favourably with the material's properties, potentially resulting in lower strain energy.

Finally, Fig. 15 shows the maximum principal stress (MPa) versus force (N) for all three groove designs. The results indicate that the vertical grooves design consistently had lower mean principal stress values compared to the other designs, indicating that this design has a lower risk of failure due to stress concentration.

In summary, the results of the simulations suggest that groove design has a significant impact on the mechanical behaviour of solid hip implants. Among the three designs tested, the solid femoral head having vertical grooves consistently had better overall properties, with lower mean total deformation and mean principal stress values compared to the other designs. However, the horizontal grooves design had the highest mean strain energy values, suggesting that it may have the ability to absorb more energy under loading conditions.

The study investigated the effect of grooves on the stress distribution of a femoral head. For the femoral head without grooves, the maximum total deformation increased from 0.0161421 mm to 0.0807104 mm as the applied force increased from 500 N to 2500 N. The maximum shear stress increased from 59.951 MPa to 299.754 MPa, while the maximum strain energy increased from 0.0012746 mJ to 0.0318647 mJ, and the maximum principal stress increased from 115.618 MPa to 578.091 MPa.

For the femoral head with vertical grooves, the maximum total deformation increased from 0.0137140 mm to 0.0685707 mm as the applied force increased from 500 N to 2500 N. The maximum shear stress increased from 60.117 MPa to 300.586 MPa, while the maximum strain energy increased from 0.0013881 mJ to 0.0347018 mJ, and the maximum principal stress increased from 89.433 MPa to 447.167 MPa.

For the femoral head with horizontal grooves, the maximum total deformation increased from 0.0162731 mm to 0.0813479 mm as the applied force increased from 500 N to 2500 N. The maximum shear stress increased from 60.938 MPa to 308.280 MPa, while the maximum strain energy increased from 0.0017591 mJ to 0.0439788 mJ, and the maximum principal stress increased from 115.355 MPa to 576.773 MPa.

Overall, the results show that the presence of grooves in the femoral head reduces the maximum stress values and the deformation of the head. Among the three groove designs, the vertical groove design showed the best performance in reducing the maximum stress values and the deformation of the femoral head.

The results of this study highlight the importance of carefully designing and testing hip implants under different loading conditions to ensure their safety and effectiveness. Although the hip implant was able to withstand the applied loads without failure, the areas of high stress concentration observed in the femoral stem and acetabular cup emphasize the need for further research to optimize the design and materials of hip implants to improve their longevity and patient outcomes. The below section gives a detail explanation regarding the optimization technique used in this research.

3.2. Optimization

In this study, simulation results were analysed using Minitab software to investigate the effect of two factors on the response variables related to the mechanical behaviour of a material. The experimental design was a general full factorial design with two factors, namely 'Groove Design' and 'Force'. The first factor, 'Groove Design,' had three levels: vertical grooves, horizontal grooves, and no grooves, while the second factor, 'Force,' had levels ranging from 500 N to 2500 N with an increment of 400 N. The response variables were Total Deformation Maximum (mm), Shear Stress Maximum (MPa), Strain Energy Maximum (mJ), and Principal Stress Maximum (MPa). The General Linear Model analysis was carried out in Minitab, and the ANOVA results indicated that all the models were acceptable. Main effect plots were then generated to compare the results, showing the effect of each factor on the response variables. These plots provided insight into the optimal combination of factors that lead to the best mechanical behaviour of the material.

The statistical analysis of the Total Deformation Maximum (mm) response variable showed significant effects of both the Groove Design and Force factors. The P-value for Groove Design was 0.000, indicating a significant effect on the Total Deformation Maximum (mm) response variable. Similarly, the P-value for Force was 0.000, indicating a significant effect on Total Deformation Maximum (mm). The F-values of Groove Design and Force were 24.13 and 342.17, respectively, further indicating the significant effects of these factors on the response variable. The Analysis of Variance using General Linear Model for Total Deformation Maximum (mm) versus Groove Design, Force is shown in Table 1. The model summary reveals an Adjusted R^2 value that is relatively high, indicating that a significant proportion of the variation in the Total Deformation Maximum (mm) response variable can be explained by the model. The Adjusted R^2 value is adjusted for the number of predictors in the model relative to the number of observations, which further strengthens the validity of the model. Table 2 displays the model summary of the General Linear Model analysis that was conducted to investigate the relationship between Total Deformation Maximum (mm) and the factors of Groove Design and Force. The model summary provides important information regarding the overall effectiveness of the model in explaining the variation in the response variable. This information can be used to assess the validity of the model and to determine the significance of the effects of the factors on the response variable.

The Regression equation for maximum total deformation is shown in equation (1).

$$\begin{aligned}\text{Total Deformation Maximum (mm)} = {} & 0.046127 + 0.002686\ \text{Groove Design Horizontal Grooves} + 0.002299\ \text{Groove Design No Grooves} \\ & - 0.004985\ \text{Groove Design Vertical Grooves} \\ & - 0.03075\ \text{Force\_500} - 0.01845\ \text{Force\_900} - 0.00615\ \text{Force\_1300} \\ & + 0.00615\ \text{Force\_1700} + 0.01845\ \text{Force\_2100} \\ & + 0.03075\ \text{Force\_2500}\end{aligned} \quad (1)$$

From above equation, it is observed that the groove design has significant role in reducing the total deformation (mm) followed increase in force(N).

For maximum shear stress, P value of groove design was 0.000 and F-value of groove design was 24.11. Whereas P value of force was 0.000 and F-value of groove design was 39090.09. The F-value of force of maximum shear stress is dominating in this region. Analysis of Variance using General Linear Model for Shear Stress Maximum (MPa) versus Groove Design, Force is shown in Table 3.

Table 1
Analysis of variance of general linear model for total deformation maximum (mm) versus groove design, force.

Source	DF	Seq SS	Contribution	Adj SS	Adj MS	F-Value	P-Value
Groove Design	2	0.000224	2.73 %	0.000224	0.000112	24.13	0.000
Force	5	0.007943	96.71 %	0.007943	0.001589	342.17	0.000
Error	10	0.000046	0.57 %	0.000046	0.000005		
Total	17	0.008213	100.00 %				

Table 2
Model summary of general linear model for total deformation maximum (mm) versus groove design, force.

S	R-sq	R-sq(adj)	PRESS	R-sq(pred)	AICc	BIC
0.0021547	99.43 %	99.04 %	0.0001504	98.17 %	−140.04	−154.53

Table 3
Analysis of variance of general linear model for shear stress maximum (MPa) versus groove design, force.

Source	DF	Seq SS	Contribution	Adj SS	Adj MS	F-Value	P-Value
Groove Design	2	30	0.02 %	30	15.1	24.11	0.000
Force	5	122316	99.97 %	122316	24463.2	39090.09	0.000
Error	10	6	0.01 %	6	0.6		
Total	17	122352	100.00 %				

The model summary shows that Adjusted R^2, the percentage of the variation in the response that is explained by the model, adjusted for the number of predictors in the model relative to the number of observations are also high. The model summary of General Linear Model: Shear Stress Maximum (MPa) versus Groove Design, Force is shown in Table 4.

The Regression equation for maximum shear stress is shown in equation (2).

$$\text{Shear Stress Maximum (MPa)} = \begin{matrix} 181.006 + 1.808\ \text{Groove Design Horizontal Grooves} \\ - 1.154\ \text{Groove Design No Grooves} - 0.654\ \text{Groove Design Vertical} \\ \text{Grooves} - 120.671\ \text{Force\_500} - 72.402\ \text{Force\_900} \\ - 24.134\ \text{Force\_1300} + 24.134\ \text{Force\_1700} + 72.402\ \text{Force\_2100} \\ + 120.671\ \text{Force\_2500} \end{matrix} \quad 2 \qquad (2)$$

From above equation, it is observed that the groove design has significant role in reducing the shear stress (MPa) followed by Force (N).

For maximum strain energy, P value of groove design was 0.007 and F-value of groove design was 8.46. Whereas P value of force was 0.000 and F-value of groove design was 101.47. The F-value of force of maximum strain energy is dominating in this region. Analysis of Variance using General Linear Model for Strain Energy Maximum (mJ) versus Groove Design, Force is shown in Table 5. The model summary shows that Adjusted R^2, the percentage of the variation in the response that is explained by the model, adjusted for the number of predictors in the model relative to the number of observations are also high. The model summary of General Linear Model: Strain Energy Maximum (mJ) versus Groove Design, Force is shown in Table 6.

The Regression Equation for maximum strain energy is shown in equation (3).

$$\begin{aligned} \text{Strain energy maximum (mJ)} = {} & 0.016017 + 0.003099\ \text{Groove design Horizontal Grooves} - 0.002166\ \text{Groove design No Grooves} \\ & - 0.000933\ \text{Groove design Vertical Grooves} - 0.01454\ \text{Force\_500} \\ & - 0.01124\ \text{Force\_900} - 0.00605\ \text{Force\_1300} + 0.00102\ \text{Force\_1700} \\ & + 0.00998\ \text{Force\_2100} + 0.02083\ \text{Force\_2500} \end{aligned} \quad 3 \qquad (3)$$

From above equation, it is observed that the groove design has major role in improving the strain energy (mJ) by the increase in Force(N).

For maximum principal stress, P value of groove design was 0.000 and F-value of groove design was 24.11. Whereas P value of force was 0.000 and F-value of groove design was 151.24. The F-value of force of maximum principal stress is dominating in this region. Analysis of Variance using General Linear Model for principal stress maximum (MPa) versus Groove Design, Force is shown in Table 7. The model summary shows that Adjusted R^2, the percentage of the variation in the response that is explained by the model, adjusted for the number of predictors in the model relative to the number of observations are also high. The model summary of General Linear Model: Principal stress maximum (MPa) versus Groove Design, Force is shown in Table 8.

The Regression Equation for maximum Principal stress is shown in equation (4).

$$\begin{aligned} \text{Principal stress Maximum (MPa)} = {} & 320.41 + 25.66\ \text{Groove design Horizontal Grooves} + 26.45\ \text{Groove design No Grooves} \\ & - 52.11\ \text{Groove design Vertical Grooves} - 213.6\ \text{Force\_500} \\ & - 128.2\ \text{Force\_900} - 42.7\ \text{Force\_1300} + 42.7\ \text{Force\_1700} \\ & + 128.2\ \text{Force\_2100} + 213.6\ \text{Force\_2500} \end{aligned} \quad 4 \qquad (4)$$

From above equation, it is observed that the groove design has significant role in reducing the principal stress (MPa) by positive

Table 4
Model summary of general linear model for shear stress maximum (MPa) versus groove design, force.

S	R-sq	R-sq(adj)	PRESS	R-sq(pred)	AICc	BIC
0.791085	99.99 %	99.99 %	20.2764	99.98 %	72.57	58.08

Table 5
Analysis of variance of general linear model for strain energy maximum (mJ) versus groove design, force.

Source	DF	Seq SS	Contribution	Adj SS	Adj MS	F-Value	P-Value
Groove Design	2	0.000091	3.17 %	0.000091	0.000046	8.46	0.007
Force	5	0.002728	94.96 %	0.002728	0.000546	101.47	0.000
Error	10	0.000054	1.87 %	0.000054	0.000005		
Total	17	0.002872	100.00 %				

Table 6
Model summary of general linear model for strain energy maximum (mJ) versus groove design, force.

S	R-sq	R-sq(adj)	PRESS	R-sq(pred)	AICc	BIC
0.0023186	98.13 %	96.82 %	0.0001742	93.94 %	−137.40	−151.89

Table 7
Analysis of Variance of General Linear Model for Principal stress maximum (MPa) versus Groove Design, Force.

Source	DF	Seq SS	Contribution	Adj SS	Adj MS	F-Value	P-Value
Groove Design	2	24437	5.92 %	24437	12218.6	24.11	0.000
Force	5	383264	92.85 %	383264	76652.9	151.24	0.000
Error	10	5068	1.23 %	5068	506.8		
Total	17	412770	100.00 %				

Table 8
Model Summary of General Linear Model for Principal stress maximum (MPa) versus Groove Design, Force.

S	R-sq	R-sq(adj)	PRESS	R-sq(pred)	AICc	BIC
22.5132	98.77 %	97.91 %	16421.8	96.02 %	193.11	178.62

variation of Force(N).

Overall, these results suggest that both Groove Design and Force have significant effects on Total Deformation Maximum (mm), Shear Stress Maximum (MPa), Strain Energy Maximum (mJ), and Principal Stress Maximum (MPa). These findings can be utilized in optimizing the design of mechanical components and materials to achieve the desired level of deformation.

3.2.1. Main effects plot

To gain a better understanding of the effect of groove design and force on various response variables, main effects plots were generated for maximum total deformation (mm), maximum shear stress (MPa), maximum strain energy (mJ), and maximum principal stress (MPa) of the femoral head. Three groove designs were considered: horizontal grooves, vertical grooves, and no grooves, while force levels ranged from 500 N to 2500 N with an increment of 400 N.

The main effect plot for maximum total deformation showed that vertical grooves had a lower mean deformation compared to the other groove designs, suggesting that this design may be effective in reducing deformation under high forces. However, the main effect plot for maximum shear stress showed no significant differences among the groove designs, indicating that the presence or absence of grooves did not significantly influence shear stress.

The main effect plot for maximum strain energy indicated that horizontal grooves had the highest strain energy, while vertical grooves had a higher strain energy value compared to the solid femoral head with no grooves. This result suggests that the presence of grooves, particularly horizontal ones, could potentially enhance the energy absorption capacity of the femoral head.

The main effect plot for maximum principal stress showed that vertical grooves were significantly better with a lower mean principal stress value, indicating that this design may help reduce stress concentrations in the femoral head.

In addition, a positive linear correlation was observed between the value of force and the response variables. Figs. 16–19 illustrate the relationship between the mean of the response variables and groove design and force, including maximum total deformation (mm), maximum shear stress (MPa), maximum strain energy (mJ), and maximum principal stress (MPa), respectively. These figures provide a visual representation of the trends observed in the main effects plots, and can help in optimizing the design of femoral head implants for improved mechanical performance.

Fig. 16 shows the relation between mean of maximum total deformation (mm) versus groove design and force (N). The relation between maximum shear stress (mm) versus groove design and force (N) is indicated in Fig. 17. Fig. 18 represents the relation between mean of maximum strain energy (mJ) versus groove design and force (N). The relation between mean of maximum principal stress (MPa) versus groove design and force (N) is shown in Fig. 19.

After performing the simulation and analysis of the data using Minitab software, the following conclusions can be drawn. The results show that the groove design has a significant impact on the mechanical behaviour of solid hip implants. The main effect plots indicate that the choice of groove design affects the maximum total deformation, maximum strain energy, and maximum principal

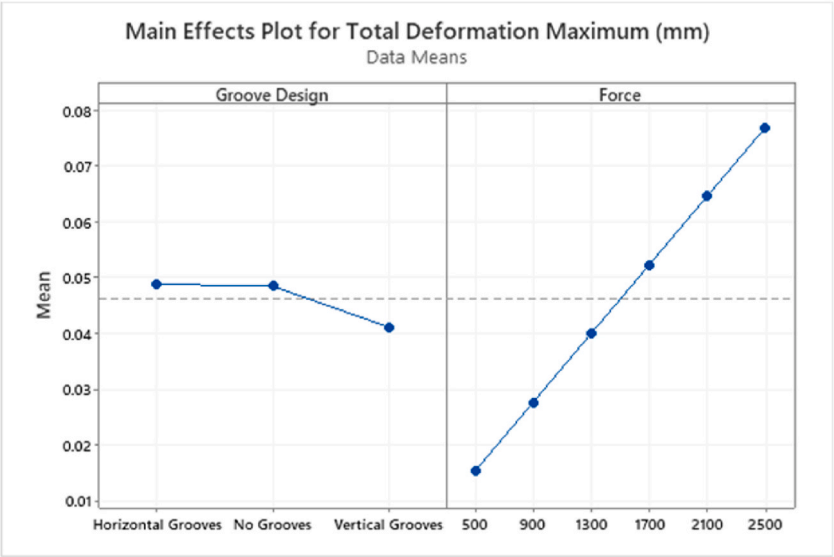

Fig. 16. Main effect plot for Total deformation maximum (mm) Vs Groove designs, Force (N).

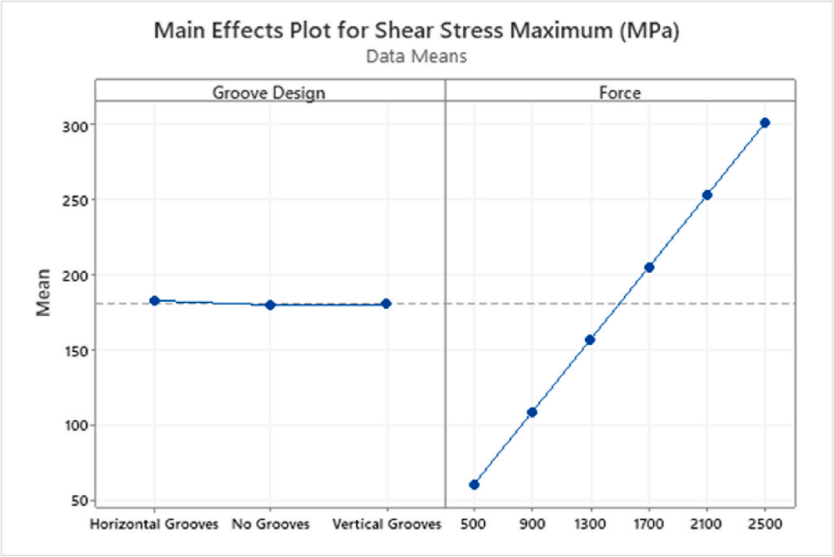

Fig. 17. Main effect plot for shear stress maximum (mm) Vs Groove designs, Force (N).

stress of the femoral head. Among the designs tested, the solid femoral head having vertical grooves exhibited the best overall mechanical properties with lower mean deformation, higher strain energy, and lower mean principal stress values. However, there was no significant effect of groove design on maximum shear stress. The positive correlation between force and response variables indicates that the force applied to the femoral head increases the response variables linearly. In conclusion, the choice of groove design plays an important role in determining the mechanical properties of solid hip implants, and the design with vertical grooves shows promising results for future development of hip implants.

While this study offers valuable insights into the optimization of femoral head design for solid hip implants, it is important to address certain limitations. One notable limitation is the challenge of obtaining direct experimental validation for the numerical simulations, primarily due to the intricate and multifaceted nature of hip implant biomechanics. To address this, authors are actively exploring opportunities to validate the numerical results against available experimental data, where applicable. However, it is worth noting that finite element analysis (FEA) techniques, employed in this study, are well-established and validated through extensive benchmarking against known experimental outcomes in the field.

Another key consideration is the difference between the numerical load applied in the simulations and the in vivo load experienced

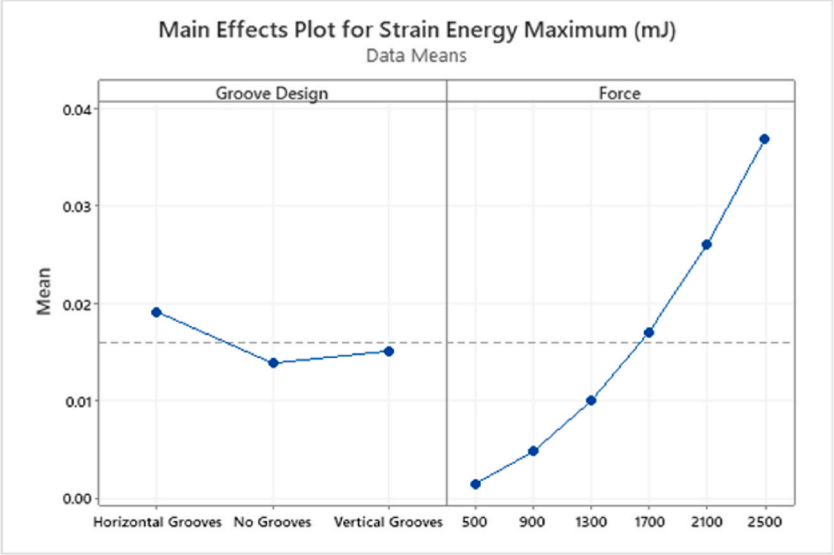

Fig. 18. Main effect plot for strain energy maximum (mm) Vs Groove designs, Force (N).

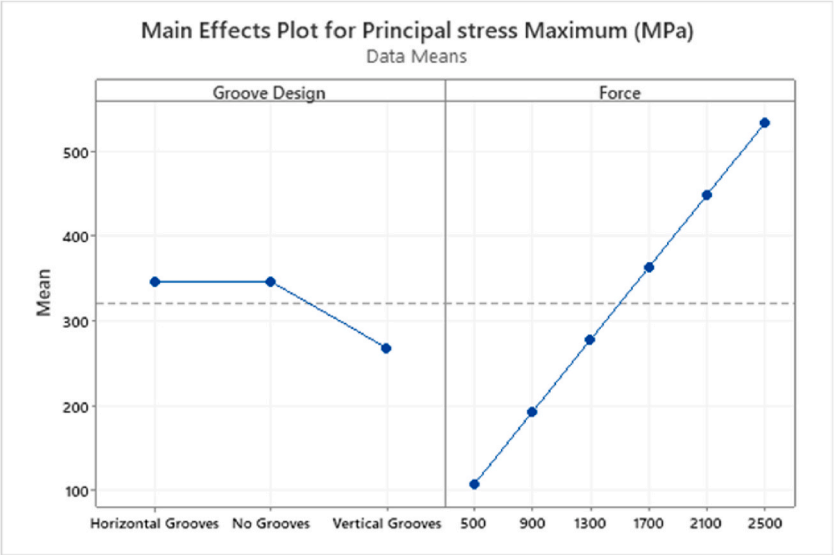

Fig. 19. Main effect plot for principal stress maximum (mm) Vs Groove designs, Force (N).

at the bone-implant interface. Authors acknowledge that in vivo loads can vary considerably due to patient-specific factors, activities, and physiological conditions. While the numerical simulations provide valuable insights into implant performance under controlled loading conditions, the applicability of these findings to individual patient scenarios may require further investigation and customization. Authors emphasize the importance of considering these factors when interpreting and applying the results in a clinical context.

4. Conclusion

The study investigated the effect of groove designs on the mechanical behaviour of the femoral head. Three different groove designs, namely no grooves, vertical grooves, and horizontal grooves, were considered, and their mechanical behaviour was analysed under different applied forces ranging from 500 N to 2500 N. Ansys static structural analysis was used to determine the values for Maximum Total Deformation, Maximum Shear Stress, Maximum Strain Energy, and Maximum Principal Stress after running the simulations.

Results shows that the groove designs significantly affect the mechanical behaviour of the femoral head. The presence of grooves

reduced the shear stress and maximum principal stress values, which indicates that the grooves can help in reducing the stress concentration and hence can improve the mechanical behaviour of the femoral head. Moreover, the strain energy and total deformation values also decreased with the groove designs, which indicates that the grooves can help in reducing the deformation and energy absorption capacity of the femoral head. The vertical groove design exhibited the lowest total deformation and stress distribution among the three designs, while the no groove design showed the highest values. The horizontal groove design was found to be intermediate in terms of performance. The optimization process using general full factorial design revealed that the optimal groove design was a vertical model with a depth of 1 mm and a width of 3 mm.

The study acknowledges the limitations associated with its simplified loading conditions, which may not fully replicate the complexity of in vivo loading experienced by hip implants. Future research should explore more realistic loading scenarios, considering factors like muscle forces, body weight distribution, and joint kinematics, to achieve a comprehensive understanding of hip implant performance.

5. Future scope

This study lays the foundation for an extended exploration into the influence of surface groove designs on the mechanical behaviour of the femoral head in hip implant designs. Future investigations can encompass a detailed analysis of different groove designs, including variations in key geometric parameters such as groove depth, width, and spacing. Additionally, to complement the numerical simulations, experimental methods can be employed to investigate the impact of groove designs on wear behaviour, providing a holistic understanding of implant performance. Furthermore, the knowledge gleaned from this study can serve as a stepping stone for the development of optimized groove patterns tailored to enhance the mechanical behaviour of the femoral head. By mitigating stress concentrations and wear, these optimized designs hold the potential to reduce the risk of implant failure in patients undergoing hip replacement surgery, ultimately improving patient outcomes and implant longevity.

In essence, this study not only offers valuable insights into the role of groove designs but also paves the way for future research endeavours that aim to refine implant design strategies and advance the field of biomechanics in hip replacement surgery.

Funding

This research is supported by the Research Office of UAE University.

Data availability statement

The authors have not deposited the data associated with this study into a publicly available repository. The data used in this study is confidential and, as such, has not been made publicly accessible.

CRediT authorship contribution statement

Asarudheen Abdudeen: Writing – review & editing, Writing – original draft, Visualization, Validation, Software, Resources, Project administration, Methodology, Investigation, Formal analysis, Data curation, Conceptualization. **Jaber E. Abu Qudeiri:** Software, Resources, Project administration, Funding acquisition, Formal analysis. **Ansar Kareem:** Software, Formal analysis, Data curation.

Declaration of competing interest

The authors declare that they have no known competing financial interests or personal relationships that could have appeared to influence the work reported in this paper.

References

[1] J. Abu Qudeiri, A. Abdudeen, M.R. Sahadevan, Hip Implant with Reduced Wear, 2023.
[2] S.M. Kurtz, K.L. Ong, E. Lau, K.J. Bozic, Impact of the economic downturn on total joint replacement demand in the United States: updated projections to 2021, JBJS, J. Bone Joint Surg. 96 (2014) 624–630.
[3] E. Lenguerrand, M.R. Whitehouse, A.D. Beswick, S.K. Kunutsor, P. Foguet, M. Porter, A.W. Blom, N.J.R. for England, N. Wales, Risk factors associated with revision for prosthetic joint infection following knee replacement: an observational cohort study from England and Wales, Lancet Infect. Dis. 19 (2019) 589–600.
[4] P.N. Ramkumar, C.T. Chu, J.D. Harris, A. Athiviraham, M.A. Harrington, D.L. White, D.H. Berger, A.D. Naik, L.T. Li, Causes and rates of unplanned readmissions after elective primary total joint arthroplasty: a systematic review and meta-analysis, Am. J. Orthoped. 44 (2015) 397–405.
[5] K.T. Mäkelä, O. Furnes, G. Hallan, A.M. Fenstad, O. Rolfson, J. Kärrholm, C. Rogmark, A.B. Pedersen, O. Robertsson, W. Annette, The benefits of collaboration: the nordic arthroplasty register association, EFORT Open Rev 4 (2019) 391.
[6] M.C. Hochberg, Mortality in osteoarthritis, Clin. Exp. Rheumatol. 26 (2008) S120.
[7] N. guideline NG157. Joint replacement (primary): hip, knee and shoulder, Methods, 2020. NICE, ISBN 978-1-4731-3722-6.
[8] K.-S. Shih, C.-C. Hsu, T.-P. Hsu, S.-M. Hou, C.-K. Liaw, Biomechanical analyses of static and dynamic fixation techniques of retrograde interlocking femoral nailing using nonlinear finite element methods, Comput. Methods Progr. Biomed. 113 (2014) 456–464.
[9] J. Henckel, R. Richards, K. Lozhkin, S. Harris, F.M.R. y Baena, A.R.W. Barrett, J.P. Cobb, Very low-dose computed tomography for planning and outcome measurement in knee replacement: the imperial knee protocol, J Bone Joint Surg Br 88 (2006) 1513–1518.

[10] R. Huiskes, H. Weinans, H.J. Grootenboer, M. Dalstra, B. Fudala, T.J. Slooff, Adaptive bone-remodeling theory applied to prosthetic-design analysis, J. Biomech. 20 (1987) 1135–1150.
[11] N. Patsiogiannis, N.K. Kanakaris, P. V Giannoudis, Periprosthetic hip fractures: an update into their management and clinical outcomes, EFORT Open Rev 6 (2021) 75.
[12] D.C. Montgomery, G.C. Runger, N.F. Hubele, Engineering Statistics, John Wiley and Sons, Inc, New York, 1998, pp. 135–248.
[13] G. Nazari, D. Diep, J.C. MacDermid, The state of trial registrations in the field of Orthopaedics in years 2015–2020. A meta-epidemiological study, Osteoarthr Cartil Open 3 (2021) 100215.
[14] M. Kumar, A. Kumar, H.N.S. Yadav, A. Alok, M. Das, Abrasive based finishing method applied on biomedical implants: a review, Mater. Today: Proc. 47 (2021) 3985–3992.
[15] J.E.A. Qudeiri, A. Abdudeen, M.R. Sahadevan, Numerical investigation on the wear characteristics of hip implant under static loading, Heliyon 10 (2024), 1-13.
[16] H. Kurokawa, A. Taniguchi, S. Morita, Y. Takakura, Y. Tanaka, Total ankle arthroplasty incorporating a total talar prosthesis: a comparative study against the standard total ankle arthroplasty, Bone Joint Lett. J 101 (2019) 443–446.
[17] J.D. Spratt, L.R. Salkowski, M. Loukas, T. Turmezei, J. Weir, P.H. Abrahams, Weir & Abrahams' Imaging Atlas of Human Anatomy E-Book, Elsevier Health Sciences, 2020.
[18] C.A. Engh, J.D. Bobyn, A.H. Glassman, Porous-coated hip replacement. The factors governing bone ingrowth, stress shielding, and clinical results, J Bone Joint Surg Br 69 (1987) 45–55.
[19] M. Spector, M.D. Ries, R.B. Bourne, W.S. Sauer, M. Long, G. Hunter, Wear performance of ultra-high molecular weight polyethylene on oxidized zirconium total knee femoral components, JBJS 83 (2001) S80–S86.
[20] W.H. Harris, Osteolysis and particle disease in hip replacement: a review, Acta Orthop. Scand. 65 (1994) 113–123.
[21] S.L. Smith, D. Dowson, A.A.J. Goldsmith, The effect of femoral head diameter upon lubrication and wear of metal-on-metal total hip replacements, Proc. Inst. Mech. Eng. H 215 (2001) 161–170.
[22] N.D. Clement, L.C. Biant, S.J. Breusch, Total hip arthroplasty: to cement or not to cement the acetabular socket? A critical review of the literature, Arch. Orthop. Trauma Surg. 132 (2012) 411–427.
[23] S. Ghosh, S. Sanghavi, P. Sancheti, Metallic biomaterial for bone support and replacement, in: Fundamental Biomaterials: Metals, Elsevier, 2018, pp. 139–165.
[24] H.S. Gandhi, The exploitation of correlation between mechanobiology of bone fracture healing, osteosynthesis, and biomaterials for optimization process and design principles to develop ame, J. Long Term Eff. Med. Implants 33 (2023) 35–86.
[25] M. Zhou, H. Sun, Y. Gan, C. Ji, Y. Chen, Y. Lu, J. Lin, Q. Wang, Tuning the corrosion resistance, antibacterial activity, and cytocompatibility by constructing grooves on the surface of Ti6al4v3cu alloy, Antibacterial Activity, and Cytocompatibility by Constructing Grooves on the Surface of Ti6al4v3cu, Alloy 36 (2023) 1979–1998.
[26] K. Moghadasi, M.S.M. Isa, M.A. Ariffin, S. Raja, B. Wu, M. Yamani, M.R. Bin Muhamad, F. Yusof, M.F. Jamaludin, M.S. bin Ab Karim, A review on biomedical implant materials and the effect of friction stir based techniques on their mechanical and tribological properties, J. Mater. Res. Technol. 17 (2022) 1054–1121.
[27] U. Mueller, S. Braun, S. Schroeder, R. Sonntag, J.P. Kretzer, Same same but different? 12/14 stem and head tapers in total hip arthroplasty, J. Arthroplasty 32 (2017) 3191–3199.
[28] O.K. Muratoglu, C.R. Bragdon, D.O. O'Connor, M. Jasty, W.H. Harris, A novel method of cross-linking ultra-high-molecular-weight polyethylene to improve wear, reduce oxidation, and retain mechanical properties: recipient of the 1999 HAP Paul Award, J. Arthroplasty 16 (2001) 149–160.
[29] O. Hussain, B. Ahmad, S. Saleem, Analysis of tribological behavior of medical-grade UHMW polyethylene under dry and lubricated conditions with human body fluids using Taguchi and GRA techniques, J. Thermoplast. Compos. Mater. 35 (2022) 1940–1956.
[30] J. Jamari, M.I. Ammarullah, A.P.M. Saad, A. Syahrom, M. Uddin, E. van der Heide, H. Basri, The effect of bottom profile dimples on the femoral head on wear in metal-on-metal total hip arthroplasty, J. Funct. Biomater. 12 (2021) 38.
[31] H.N. Beidokhti, D. Janssen, S. van de Groes, J. Hazrati, T. Van den Boogaard, N. Verdonschot, The influence of ligament modelling strategies on the predictive capability of finite element models of the human knee joint, J. Biomech. 65 (2017) 1–11.
[32] P. Goshulak, S. Samiezadeh, M.S.R. Aziz, H. Bougherara, R. Zdero, E.H. Schemitsch, The biomechanical effect of anteversion and modular neck offset on stress shielding for short-stem versus conventional long-stem hip implants, Med. Eng. Phys. 38 (2016) 232–240.
[33] C. Luo, X.-D. Wu, Y. Wan, J. Liao, Q. Cheng, M. Tian, Z. Bai, W. Huang, Femoral stress changes after total hip arthroplasty with the ribbed prosthesis: a finite element analysis, BioMed Res. Int. 2020 (2020).
[34] Y. Zhao, L. Wang, Y. Bao, R. Xu, S. He, Finite element analysis of optimal design of distal geometry of cementless femoral prosthesis, Niger. J. Clin. Pract. 25 (2022) 1476–1483.
[35] W.H. Kim, J.-C. Lee, D. Lim, Y.-K. Heo, E.-S. Song, Y.-J. Lim, B. Kim, Optimized dental implant fixture design for the desirable stress distribution in the surrounding bone region: a biomechanical analysis, Materials 12 (2019) 2749.
[36] A. Abdudeen, J.E. Abu Qudeiri, A. Kareem, A.K. Valappil, Latest developments and insights of orthopedic implants in biomaterials using additive manufacturing technologies, J. Manuf. Mater. Process. 6 (2022) 162.
[37] E. Askari, P. Flores, D. Dabirrahmani, R. Appleyard, A review of squeaking in ceramic total hip prostheses, Tribol. Int. 93 (2016) 239–256.